

Elastoplastic Analysis of Circular Tunnel in Saturated Ground Under Different Load Conditions

Panpan Zhai^{1, 2} and Ping Xu^{1, 2, *}

Abstract: When a tunnel is excavated below the groundwater table, groundwater flows in through the excavated wall of the tunnel and seepage forces act on it. These forces significantly affect the ground reaction curve, which is defined as the relationship between the internal pressure and radial displacement of the tunnel wall. This study investigates analytical solutions for seepage forces acting on the lining of a circular tunnel under steady-state groundwater flow. Considering the tunnel's construction or service period and boundary conditions, the direction of maximum principal stress changes, and the input stress of the Mohr-Coulomb criterion varies. The stress distribution and yield range of the surrounding soils and linings are studied. The first, second, and third critical inner pressures are defined and evaluated. The influence of the seepage field on the plastic radius, first critical pressure, and stress distribution of the tunnel is analyzed. It is shown that during the construction period, the seepage force promotes the expansion of the yield area, whereas during the service period, the opposite is the case. The first critical pressure increases nearly linearly with the distant water pressure. The radial stress distribution decreases clearly in comparison with that when the seepage force is not considered, and the reduction is more prominent when internal pressure increases. The tangential stress distribution increases clearly compared with that when the seepage force is not considered.

Keywords: Tunnel lining, surrounding soils, elastoplastic analysis, critical pressure, plastic radius, seepage force.

1 Introduction

The seepage force in porous media deforms and damages soils and rocks, and its influence is distinct on different soils or rock masses. For poroelastic media, fracture behavior is controlled by the phase field model [Zhou, Rabczuk and Zhuang (2018); Zhou and Xia (2018); Zhou, Zhuang and Rabczuk (2018); Zhou, Zhuang, Zhu et al. (2018)]. Moreover, fracture propagation is driven by elastic energy, where the phase field is used as an interpolation function to transition the property of the fluid from the intact medium to the fully broken one. The phase field method for dynamic cracks in a single-

¹ College of Water Conservancy & Environmental Engineering, Zhengzhou University, Zhengzhou, 450001, China.

² National Local Joint Engineering Laboratory of Major Infrastructure Testing and Rehabilitation Technology, Zhengzhou, 450001, China.

* Corresponding Author: Ping Xu. Email: pingxu127@163.com.

phase solid has been extended for fluid-driven dynamic cracks [Zhou, Zhuang and Rabczuk (2019)]. Research on computational methods to study cracks has also been pursued in Ren et al. [Ren, Zhuang and Rabczuk (2017); Ren, Zhuang, Cai et al. (2016); Rabczuk, Zi, Bordas et al. (2010); Rabczuk and Belytschko (2004)].

When a tunnel is excavated below the groundwater table, groundwater flows in through excavated wall of the tunnel and seepage forces act on it. These seepage forces significantly affect the ground reaction curve, which is defined as the relationship between the internal pressure and radial displacement of the tunnel wall. Groundwater seepage acts on surrounding soils and linings through the seepage volume force, which affects the distribution of stress and displacement fields of the tunnel's structures. When groundwater flows into a tunnel below the groundwater table, the stress of the soil mass is the state of "the submerged weight plus seepage force." In this case, seepage forces are considered among the most influential factors, and their calculation is crucial in determining the behavior of the tunnel.

Most mast research on the ground reaction curve [Brown, Bray, Ladanyi et al. (1983); Stille, Holmberg and Nord (1989); Carranza-Torres and Fairhurst (1999, 2000); Sharan (2003); Oreste (2003)] did not consider seepage forces, and was confined to examining dry conditions. A few studies on the effects of seepage forces on the faces of tunnels and their support systems were conducted by Wood et al. [Wood (1975); Atkinson and Mair (1983); Bobet (2003)].

For deep tunnels with high water head, the influence of seepage fields cannot be ignored, and the stress distribution of the surrounding soils and linings of the tunnels exhibit prominent changes [Shin, Kim, Shin et al. (2010); Fernandez and Alvarez (1994); Lee and Nam (2001)]. In addition, with the differences in tunnel construction and service periods, the stress state of the lining and surrounding soil changes, and the selection of the maximum principal stress is very important [Ren and Zhang (2001)]. For example, during tunnel construction, radial stress is usually chosen as the maximum principal stress due to in-situ stress release [Lu, Xu, Sun et al. (2010); Jiang, Yaneda, Tanabashi et al. (2001); Carranza-Torres (2004)]. When high-pressure diversion tunnels in service usually bear relatively large internal pressure [Li, Cai, Zhuang et al. (2009)], the tunnel linings and surrounding soils also yield, and the maximum principal stress is the tangential stress in this case. Because of the transformation of the maximum principal stress, the mechanism of the influence of seepage force on the stress distribution of the lining and surrounding soil also change in different periods of the tunnel, in construction and in service. The modes of its influence on the plastic radius and critical internal pressure of the tunnel change as well.

In this paper, the circular tunnel with a lining structure in a water-rich stratum is considered. According to different periods of the tunnel in construction and service, the maximum principal stress in the Mohr-Coulomb yield criterion is reasonably selected to determine the yield range of tunnel by considering different stress boundary conditions. The influence of the seepage field on the stress distribution and plastic radius is also studied, and the stress distribution formulae of the surrounding soil and lining structure are deduced. By combining examples, the variation in the plastic radius with internal

pressure is studied, and the stress distributions of the lining and surrounding soil under different internal pressures are given.

2 Calculation of seepage force

A deep buried circular tunnel is simplified as a circular structure in infinite homogeneous elastic ground. The seepage analysis model of the lining of surrounding soil is shown in Fig. 1. Assume that a stable seepage field is formed within radius r_w ; the water head on radius r_w is h_0 (corresponding water pressure is p_{w0}), the inner and outer diameters of the lining are r_a and r_b , respectively, and the permeability coefficients of the surrounding soil and lining are k_s and k_c , respectively. Because the tunnel's axial length is much longer than the section size, it is a plane problem. The flow rate at any radius in the lining is as follows:

$$Q_c = 2\pi r k_c \frac{dp_w}{dr} \quad (1)$$

The boundary condition of Eq. (1) is

$$r = r_a, p_w = 0; \quad r = r_b, p_w = p_{w1} \quad (2)$$

where p_{w1} is water pressure on the external lining. From Eqs. (1) and (2), we can get

$$Q_c = \frac{2\pi k_c p_{w1}}{\ln r_b / r_a}, \quad r_a \leq r \leq r_b \quad (3)$$

Similarly, the flow rate at any radius in the surrounding soil can be obtained as follows:

$$Q_s = \frac{2\pi k_s (p_{w0} - p_{w1})}{\ln r_w / r_b}, \quad r_b \leq r \leq r_w \quad (4)$$

The seepage flow through each section in a steady seepage field is the same. Combining Eqs. (3) and (4), the permeation pressure at any radius in the linings and soils is calculated by

$$p_w = \begin{cases} p_{w0} \frac{k_s \ln r / r_a}{k_c \ln r_w / r_b + k_s \ln r_b / r_a}, & r_a \leq r \leq r_b \\ p_{w0} \frac{k_c \ln r / r_b + k_s \ln r_b / r_a}{k_c \ln r_w / r_b + k_s \ln r_b / r_a}, & r_b \leq r \leq r_w \end{cases} \quad (5)$$

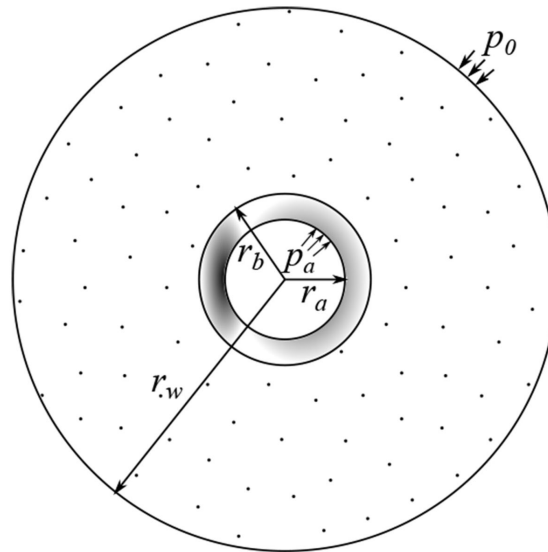


Figure 1: Stable seepage field around tunnel

3 Radial stress as maximum principal stress

For high-pressure diversion tunnels in service, the linings usually bear relatively large internal pressure. Assume that the tunnel is subjected to internal pressure p_a and the far-field stress is p_0 , and the volume force is ignored. Young's modulus and Poisson's ratio of the lining are then, respectively, E_1 and μ_1 , and the shear strength parameters are c_1 and φ_1 . Young's modulus and Poisson's ratio of the surrounding soil are E_2 and μ_2 , respectively, and the shear strength parameters are c_2 and φ_2 . The plastic radius is r_p .

During the construction of a tunnel, the stress redistribution caused by stress release leads to the yield of surrounding soil or lining structure near the excavation face because the in-situ stress release or inner support resistance is not large enough. Setting the tensile stress to positive and compressive stress to negative, $\sigma_\theta \leq \sigma_r \leq 0$, and the maximum principal stress is considered to be radial stress.

3.1 Elastic-plastic interface located in lining

This subsection considers the situation where the elastic-plastic interface is located inside the tunnel lining (see Fig. 2). The model is simplified as an axisymmetric problem. When the seepage water pressure acts on the micro-element body in the form of the volume force, the stress distribution satisfies the differential equations for equilibrium below.

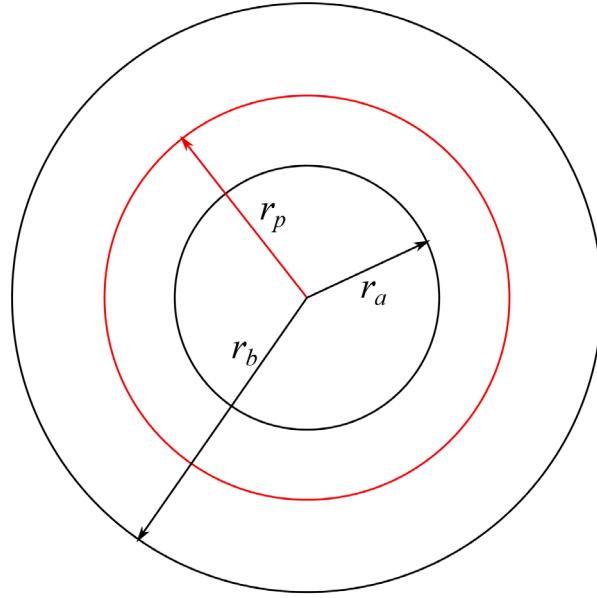


Figure 2: Plastic radius located inside the lining

$$\frac{d\sigma_r}{dr} + \frac{\sigma_r + \sigma_\theta}{r} - \beta \frac{dp_w}{dr} = 0 \quad (6)$$

In the above, σ_r and σ_θ are the radial and circumferential effective stresses, respectively, and β is the area action coefficient of seepage pressure related to the porosity of the material. For concrete materials, $\beta \in \left[\frac{2}{3} \sim 1 \right]$; for surrounding soil near failure, $\beta \approx 1$ [Xie (1994)].

In the plastic region, the stress must satisfy the Mohr–Coulomb yield condition. With $\sigma_1 = \sigma_r + \beta p_w$ and $\sigma_3 = \sigma_\theta + \beta p_w$, the yield condition can be expressed as

$$(1 + \sin \varphi) \sigma_r - (1 - \sin \varphi) \sigma_\theta = 2c \cos \varphi - 2\beta p_w \sin \varphi \quad (7)$$

Using Eq. (7), Eq. (6) can be rewritten as follows:

$$\frac{d\sigma_r}{dr} - \frac{\sigma_r}{r} \frac{2 \sin \varphi}{1 - \sin \varphi} + \frac{2c \cos \varphi - 2\beta p_w \sin \varphi}{r(1 - \sin \varphi)} - \beta \frac{dp_w}{dr} = 0 \quad (8)$$

Considering the boundary condition $(\sigma_{rc})_{r=r_a} = -p_a$ and solving differential Eq. (8), the stress distribution of the plastic region of the lining is given by

$$\sigma_{rc} = (-p_a - A) \left(\frac{r}{r_a} \right)^{\frac{2 \sin \varphi}{1 - \sin \varphi}} + \left(A - B \ln \frac{r}{r_a} \right) \quad (9)$$

where

$$\left\{ \begin{aligned} A &= \frac{c_1 \cos \varphi_1}{\sin \varphi_1} - \frac{1 - \sin \varphi_1}{\sin \varphi_1} B \\ B &= \frac{\beta p_w k_s}{k_c \ln \frac{r_w}{r_b} + k_s \ln \frac{r_b}{r_a}} \end{aligned} \right. \quad (10)$$

According to knowledge of elasticity [Timoshenko and Goodier (1969)], stress distribution in the elastic region can be calculated by considering the boundary conditions and the displacement compatibility condition of the soil lining (11):

$$\left\{ \begin{aligned} (\sigma_{rc})_{r=r_p} &= -q_{rp} & (\sigma_{rs})_{r \rightarrow \infty} &= -p_0 \\ (\sigma_{rc})_{r=r_b} &= (\sigma_{rs})_{r=r_b} & (u_{rc})_{r=r_b} &= (u_{rs})_{r=r_b} \end{aligned} \right. \quad (11)$$

where u_{rc} and u_{rs} represent the radial displacement of the lining and the surrounding soil, respectively, and q_{rp} is normal stress at the elastic-plastic interface. The stress distribution of the lining and surrounding soil in the elastic zone is calculated by

$$\left\{ \begin{aligned} \sigma_{rc} &= \frac{2(1-\mu_2)}{D} p_0 - \frac{(1-2\mu_1)n+1}{D} q_{rp} + \frac{1-n}{Dr_b^2} q_{rp} - \frac{2(1-\mu_2)}{Dr_p^2} p_0 \\ \sigma_{\theta c} &= -\frac{2(1-\mu_2)}{D} p_0 + \frac{(1-2\mu_1)n+1}{D} q_{rp} + \frac{1-n}{Dr_b^2} q_{rp} - \frac{2(1-\mu_2)}{Dr_p^2} p_0 \\ \sigma_{rs} &= \frac{(1-2\mu_2+n)r_p^2 + (n+2\mu_2-2n\mu_1-1)r_b^2}{Dr_p^2} p_0 - \frac{2n(1-\mu_1)}{D} q_{rp} - p_0 \\ \sigma_{\theta s} &= -\frac{(1-2\mu_2+n)r_p^2 + (n+2\mu_2-2n\mu_1-1)r_b^2}{Dr_p^2} p_0 + \frac{2n(1-\mu_1)}{D} q_{rp} - p_0 \end{aligned} \right. \quad (12)$$

$$\text{where } n = \frac{E_2(1+\mu_1)}{E_1(1+\mu_2)}, \quad D = \frac{(1-2\mu_1)n+1}{r_p^2} - \frac{1-n}{r_b^2}.$$

Normal stress at the elastic-plastic interface q_{rp} can be obtained using Eqs. (7) and (12) as follows:

$$q_{rp} = \frac{r_b^2 \left[2p_0(1-\mu_2)(1-\sin \varphi_1) - Dr_p^2(c_1 \cos \varphi_1 - \beta p_w \sin \varphi_1) \right]}{r_p^2 \left[(1-n)(1-\sin \varphi_1) + Dr_b^2 \right]}$$

If the plastic radius is exactly at the inner diameter of the lining, i.e., $r_p = r_a$, then $q_{rp} = p_a$. Define this internal pressure as the first critical pressure p_{cr1} , i.e., limit pressure as in-situ stress unloading causes the initial lining yield. According to Eqs. (9) and (11),

$$-q_{rp} = (-p_a - A) \left(\frac{r_p}{r_a} \right)^{\frac{2 \sin \phi}{1 - \sin \phi}} + \left(A - B \ln \frac{r_p}{r_a} \right) \quad (13)$$

The above equation is a transcendental equation of r_p that can be solved by the iterative method.

3.2 Elastic-plastic interface in soil

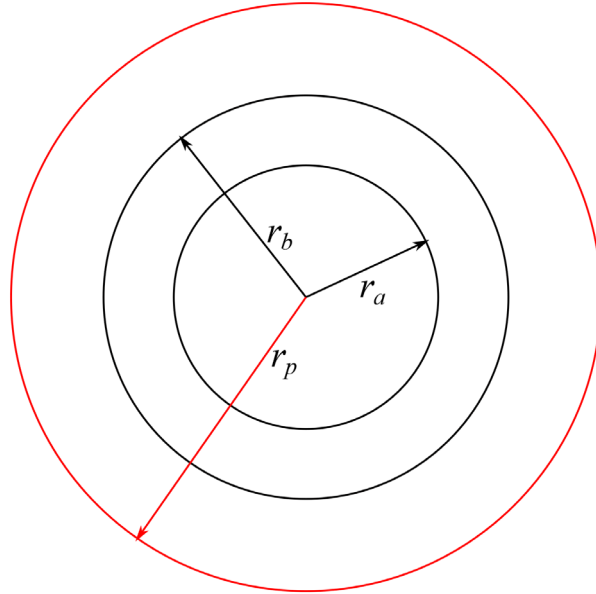


Figure 3: Plastic radius in the surrounding soil

This subsection deals with the situation where the elastic-plastic interface is located inside the surrounding soils (see Fig. 3). In the plastic region, the stress distribution should still satisfy the equilibrium condition (8) and yield criterion (7). Using boundary conditions $(\sigma_{rc})_{r=r_a} = -p_a$ and $(\sigma_{rs})_{r=r_p} = -q_{rp}$, plastic stress distribution in the lining and surrounding soil can be obtained by solving Eq. (8):

$$\sigma_{rc} = (-p_a - A) \left(\frac{r}{r_a} \right)^{\frac{2 \sin \varphi_1}{1 - \sin \varphi_1}} + \left(A - B \ln \frac{r}{r_a} \right) \quad (14)$$

$$\sigma_{rs} = (-q_{rp} - A_1) \left(\frac{r}{r_p} \right)^{\frac{2 \sin \varphi_2}{1 - \sin \varphi_2}} + \left(A_1 - \frac{1 - \sin \varphi_2}{2 \sin \varphi_2} B_1 \ln \frac{r}{r_p} \right)$$

where

$$\left\{ \begin{aligned} A_1 &= \frac{c_2 \cos \varphi_2}{\sin \varphi_2} - \frac{\beta p_{w0} k_s \ln \frac{r_b}{r_a}}{k_c \ln \frac{r_w}{r_b} + k_s \ln \frac{r_b}{r_a}} - \left(\frac{1 - \sin \varphi_2}{\sin \varphi_2} - \ln \frac{r_p}{r_b} \right) B_1 \\ B_1 &= \frac{\beta p_{w0} k_c}{k_c \ln \frac{r_w}{r_b} + k_s \ln \frac{r_b}{r_a}} \end{aligned} \right. \quad (15)$$

At the interface of the surrounding soil and the lining $(\sigma_{rc})_{r=r_b} = (\sigma_{rs})_{r=r_b}$, the plastic radius can be calculated by

$$(-p_a - A) \left(\frac{r_b}{r_a} \right)^{\frac{2 \sin \varphi_1}{1 - \sin \varphi_1}} + \left(A - B \ln \frac{r_b}{r_a} \right) = (-q_{rp} - A_1) \left(\frac{r_b}{r_p} \right)^{\frac{2 \sin \varphi_2}{1 - \sin \varphi_2}} + \left(A_1 - \frac{1 - \sin \varphi_2}{2 \sin \varphi_2} B_1 \ln \frac{r_b}{r_p} \right) \quad (16)$$

In elastic areas $r \geq r_p$. By combining boundary conditions $(\sigma_{rs})_{r=r_p} = -q_{rp}$ and $(\sigma_{rs})_{r \rightarrow \infty} = -p_0$, the stress distribution can be given by Lamé's solution in elasticity:

$$\sigma_{rs} = -\frac{r_p^2}{r^2} q_{rp} - \left(1 - \frac{r_p^2}{r^2} \right) p_0$$

$$\sigma_{\theta s} = \frac{r_p^2}{r^2} q_{rp} - \left(1 + \frac{r_p^2}{r^2} \right) p_0$$

The above formula $\sigma_{rs} + \sigma_{\theta s} = -2p_0$ holds at $r = r_p$. According to the yield condition (7), normal stress at the elastic-plastic interface q_{rp} is calculated as follows:

$$q_{rp} = p_0(1 - \sin \varphi_2) - c_2 \cos \varphi_2 + \beta p_w \sin \varphi_2.$$

4 Tangential stress as maximum principal stress

For hydraulic pressure tunnels, the inner surface of the lining bears very high water pressure while in service. When the internal water pressure is large enough or the support

pressure is too large, the plastic the structure of the tunnel can yield. In this case, the radial compressive stress is large, and circumferential compressive stress is small and can even appear as tensile stress. The maximum principal stress should thus be chosen as σ_θ . Then, $\sigma_1 = \sigma_\theta + \beta p_w$, $\sigma_3 = \sigma_r + \beta p_w$, and the Mohr–Coulomb yield condition can be expressed as

$$(1 + \sin \varphi)\sigma_\theta - (1 - \sin \varphi)\sigma_r = 2c \cos \varphi - 2\beta p_w \sin \varphi \quad (17)$$

Using Eq. (17), the differential equation for equilibrium (6) can be rewritten as follows:

$$\frac{d\sigma_r}{dr} + \frac{\sigma_r}{r} \frac{2 \sin \varphi}{1 + \sin \varphi} - \frac{2c \cos \varphi - 2\beta p_w \sin \varphi}{r(1 + \sin \varphi)} - \beta \frac{dp_w}{dr} = 0 \quad (18)$$

4.1 Elastic-plastic interface located in lining

The stress distribution of the lining in the plastic area can be obtained by solving Eq. (18) with the boundary conditions $(\sigma_{rc})_{r=r_a} = -p_a$, and introducing $c = c_1$ and $\varphi = \varphi_1$,

$$\sigma_{rc} = (-p_a - A_2) \left(\frac{r}{r_a} \right)^{\frac{2 \sin \varphi_1}{1 + \sin \varphi_1}} + \left(A_2 - B \ln \frac{r}{r_a} \right) \quad (19)$$

where

$$A_2 = \frac{c_1 \cos \varphi_1}{\sin \varphi_1} + \frac{1 + \sin \varphi_1}{\sin \varphi_1} B \quad (20)$$

In the elastic area $r \geq r_p$, according to boundary conditions at the elastic-plastic interface, can get

$$q_{rp} = \frac{r_b^2 \left[4p_0(1 - \mu_2)(1 + \sin \varphi_1) + Dr_p^2(2c_1 \cos \varphi_1 - 2\beta p_w \sin \varphi_1) \right]}{r_p^2 \left[2(1 - n)(1 + \sin \varphi_1) + 2Dr_b^2 \right]}$$

If the plastic radius is exactly at the inner diameter of the lining $r_p = r_a$, $q_{rp} = p_a$. This internal pressure is defined as the second critical pressure p_{cr2} , i.e., critical internal pressure when the lining begins to yield owing to excessive internal pressure. The plastic radius can be determined using the above equation and Eq. (19):

$$\begin{aligned} & (-p_a - A_2) \left(\frac{r_p}{r_a} \right)^{\frac{2 \sin \varphi_1}{1 + \sin \varphi_1}} + \left(A_2 - B \ln \frac{r_p}{r_a} \right) + \\ & \frac{r_b^2 \left[4p_0(1 - \mu_2)(1 + \sin \varphi_1) + Dr_p^2(2c_1 \cos \varphi_1 - 2\beta p_w \sin \varphi_1) \right]}{r_p^2 \left[2(1 - n)(1 + \sin \varphi_1) + 2Dr_b^2 \right]} = 0 \end{aligned} \quad (21)$$

4.2 Elastic-plastic interface located in soil

Considering the boundary conditions $(\sigma_{rc})_{r=r_a} = -p_a$ and $(\sigma_{rs})_{r=r_p} = -q_{rp}$, and solving Eq. (18), the plastic stress distribution in the lining and surrounding soil is obtained as follows:

$$\sigma_{rc} = (-p_a - A_2) \left(\frac{r}{r_a} \right)^{\frac{2 \sin \varphi_1}{1 + \sin \varphi_1}} + \left(A_2 - B \ln \frac{r}{r_a} \right) \quad (22)$$

$$\sigma_{rs} = (-q_{rp} - A_3) \left(\frac{r}{r_p} \right)^{\frac{2 \sin \varphi_2}{1 + \sin \varphi_2}} + \left(A_3 - \frac{1 + \sin \varphi_2}{2 \sin \varphi_2} B_1 \ln \frac{r}{r_p} \right)$$

where

$$A_3 = \frac{c_2 \cos \varphi_2}{\sin \varphi_2} - \frac{\beta p_w k_s \ln \frac{r_b}{r_a}}{k_c \ln \frac{r_w}{r_b} + k_s \ln \frac{r_b}{r_a}} + \left(\frac{1 + \sin \varphi_2}{\sin \varphi_2} + \ln \frac{r_p}{r_b} \right) B_1 \quad (23)$$

According to the contact condition between the surrounding soil and the lining $(\sigma_{rs})_{r=r_b} = (\sigma_{\theta s})_{r=r_b}$,

$$(-p_a - A_2) \left(\frac{r_b}{r_a} \right)^{\frac{2 \sin \varphi_1}{1 + \sin \varphi_1}} + \left(A_2 - B \ln \frac{r_b}{r_a} \right) = (-q_{rp} - A_3) \left(\frac{r_b}{r_p} \right)^{\frac{2 \sin \varphi_2}{1 + \sin \varphi_2}} + \left(A_3 - \frac{1 + \sin \varphi_2}{2 \sin \varphi_2} B_1 \ln \frac{r_b}{r_p} \right) \quad (24)$$

The third critical pressure can be defined by the above equation: When the internal pressure p_a continues to increase and the plastic radius extends only to the surrounding soil, this critical internal pressure is called the third critical pressure p_{cr3} . In the elastic area $\sigma_{rs} + \sigma_{\theta s} = -2p_0$, by combining the yield condition (17), normal corresponding forces on the elastic-plastic interface is calculated by

$$q_{rp} = p_0 (1 + \sin \varphi_2) + c_2 \cos \varphi_2 - \beta p_w \sin \varphi_2$$

5 Calculation of an example

According to the elastic-plastic analysis of the surrounding soil and lining, the stress state of a deep circular tunnel is clearly different under different loads. For instance, the formulae for the yield radius and stress are altered, and the seepage forces influence every coefficient of stress distribution. For a more intuitive analysis, the following examples is used, and its parameters are given in Tab. 1. The influence of these input parameters on the model is a key point, as noted in the literature [Hamdia, Ghasemi, Zhuang et al. (2018); Hamdia, Silani, Zhuang et al. (2017)].

Table 1: Geometry and material parameters of tunnel example

Parameter definition	Symbol	Unit	Value
Internal diameter of lining	r_a	m	4
External diameter of lining	r_b	m	5
Far-field stress	p_0	MPa	10
Young's modulus of lining	E_1	MPa	2.00×10^4
Poisson's ratio of lining	μ_1	-	0.167
Cohesive force of lining	c_1	MPa	5
Internal friction angle of lining	φ_1	°	45
Young's modulus of surrounding soil	E_2	MPa	2.00×10^3
Poisson's ratio of surrounding soil	μ_2	-	0.25
Cohesive force of surrounding soil	c_2	MPa	1
Internal friction angle of surrounding soil	φ_2	°	45
Permeability coefficients of surrounding soil	k_s	m/d	0.304
Permeability coefficients of lining	k_c	m/d	0
Area action coefficient of seepage pressure	β	-	0.83

If water pressure on the external lining is $p_w = \gamma_w H_w$, we can get $r_w \approx H_w = \frac{p_w}{\gamma_w}$. When internal pressure p_a is fixed, an increase in the cohesive force or internal friction angle reduces the area of the plastic region. This area increases with a decrease in the cohesive force or internal friction angle. Moreover, the far-field stress p_0 and internal pressure p_a also affect the stress distribution of the surrounding soil and lining. The results below can be obtained from the values in Tab. 1 for the Young's modulus and Poisson's ratio, which control the displacement of lining and surrounding soil. For the permeability coefficients of lining k_c , we consider a special case where the lining has a waterproof function (impervious grade P12). k_c is thus set to zero.

If the influence of the seepage force on the tunnel is not considered, i.e., $\beta = 0$, Ren's result is obtained: in-situ stress release after tunnel excavation and inner pressure $p_a = 0$, and the plastic radius is calculated as $r_p = 4.9$ m, and is located inside the lining. To reduce the yield radius, it is necessary to increase the support force p_a . When the support force reaches the first critical pressure of 4.13 MPa, the plastic area disappears. If the tunnel is a hydraulic pressure tunnel, the inner pressure p_a is very large when the tunnel is in service. If p_a is between the first critical pressure $p_{cr1} = 4.13$ MPa and the

second critical pressure $p_{cr2} = 18.55$ MPa, both the lining and the surrounding soil are in the state of elastic stress. When $p_a > 18.55$ MPa, the lining begins to yield first. If the inner pressure continues to increase and reaches $p_a = 19.5$ MPa, the plastic area extends to the interface between the lining and the surrounding soil, i.e., $r_p = 5$ m. At this stage, the excessive inner pressure leads to a change in the maximum principal stress from radial stress to tangential stress. If the inner pressure continues to increase, the plastic area extends to the surrounding soil. The results of calculation are: $p_a = 22.4$ MPa and $r_p = r_b = 5$ m. Following this, with the increase in inner pressure, the plastic area further expands in the surrounding soil.

Considering the influence of seepage water forces on the tunnel, following tunnel excavation, according to Eq. (13) if the plastic radius $r_p = 5$ m and inner pressure $p_a = 0.55$ MPa. Therefore, when $p_a = 0$, the plastic radius considering the seepage force ($r_p > 5$ m) is larger than that when this force is not considered ($r_p = 4.9$ m). With the increase in inner pressure p_a , the first critical pressure can be obtained according to Eq. (13), and $p_{cr1} = 4.1258$ MPa. If the inner pressure continues to increase, the maximum principal stress is transformed from radial to tangential stress, and the second critical pressure can be obtained according to Eq. (21). As inner pressure increases, the plastic area extends to the entire section of the lining, i.e., $r_p = r_b = 5$ m, and $p_a = 20.33$ MPa. Subsequently, the plastic radius reaches the surrounding soils and, according to Eq. (24), the third critical pressure at which the area of the surrounding soil begins to yield can be obtained as $p_{cr3} = 23.33$ MPa.

Considering the relationship between inner pressure and plastic radius, the selection of the maximum principal stress and seepage force influences plastic radius (see Fig. 4). The plastic radius decreases with an increase in the inner pressure when the maximum principal stress is not assumed to transform from radial to tangential stress. Plastic radius r_p is smaller than the lining inner diameter r_a as $p_a > p_{cr1}$, which is unreasonable. It is thus necessary to consider the transformation of the maximum principal stress from radial to tangential stress. Moreover, the curve of change in the plastic radius with internal pressure when water pressure is considered shifts to the right compared with its shape when water pressure is ignored. This shows that the inner pressure needs to offset the effect of seepage water pressure in addition to overcoming the yield stress of the lining and surrounding soil. During construction, when the inner pressure is given, the seepage water pressure promotes the expansion of the yield area. During operation, when the inner pressure is large enough, the maximum principal stress changes into tangential stress and the seepage pressure inhibits the expansion of the plastic zone.

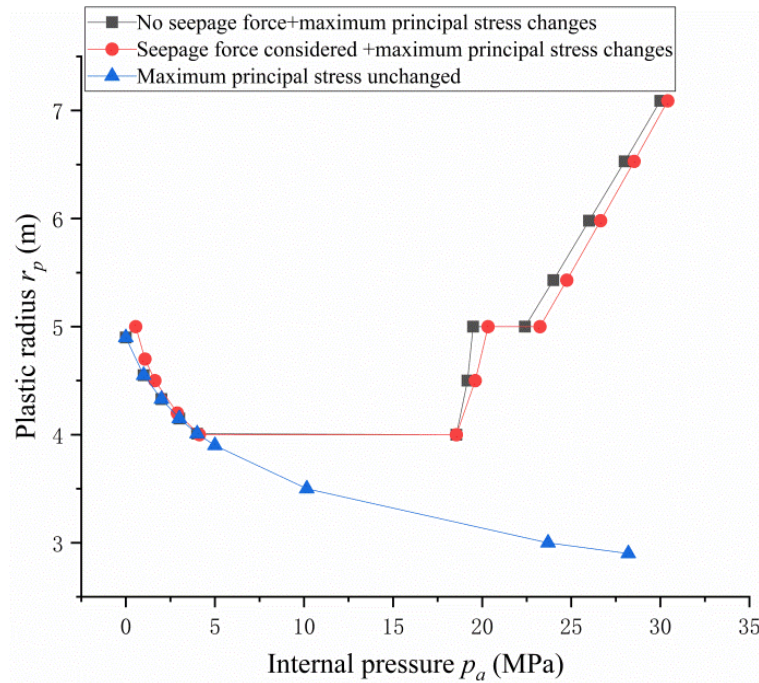


Figure 4: Relationship between plastic radius and inner pressure

During the construction of a tunnel, a redistribution of stress is caused by stress release. The calculation of the first critical pressure in tunnel construction directly affects the design of the tunnel support. The influence of seepage water pressure on the first critical pressure is considered. As shown in Fig. 5, the first critical pressure increases almost linearly with an increase in seepage water pressure. This indicates that the effect of seepage water pressure should be carefully considered during the construction of the tunnel because it plays an important role in restraining the expansion of the plastic range of the lining and surrounding soil. The variation in the second critical pressure with seepage water pressure is contrary to that of the first critical pressure, i.e., it decreases almost linearly with increase in seepage water pressure.

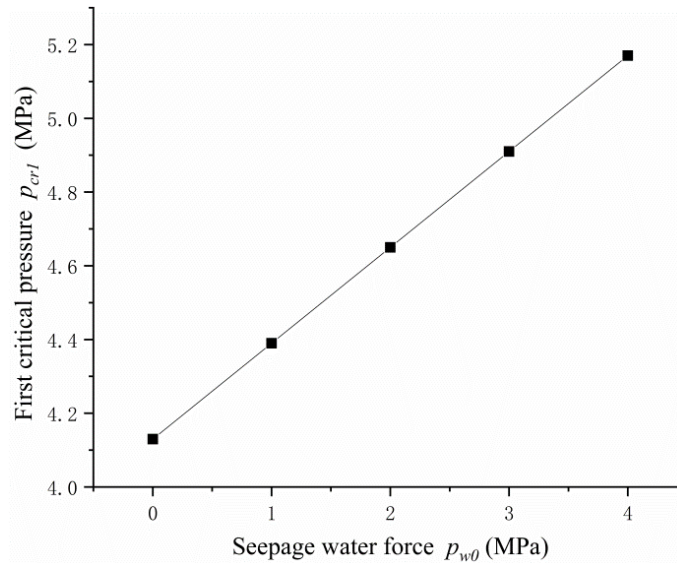
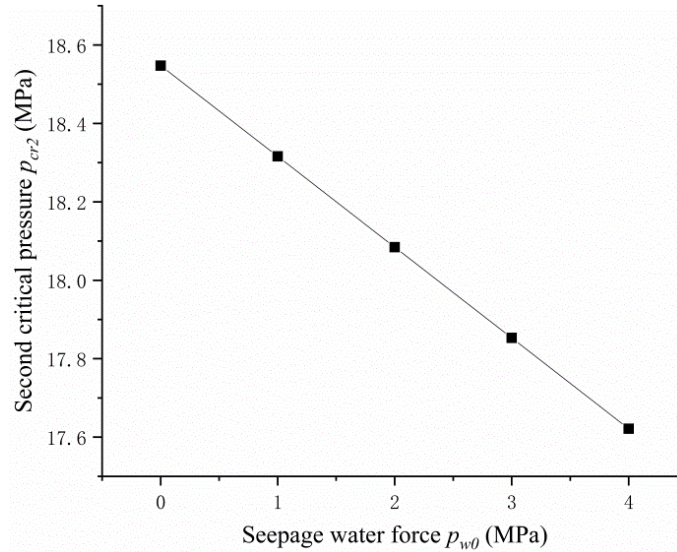
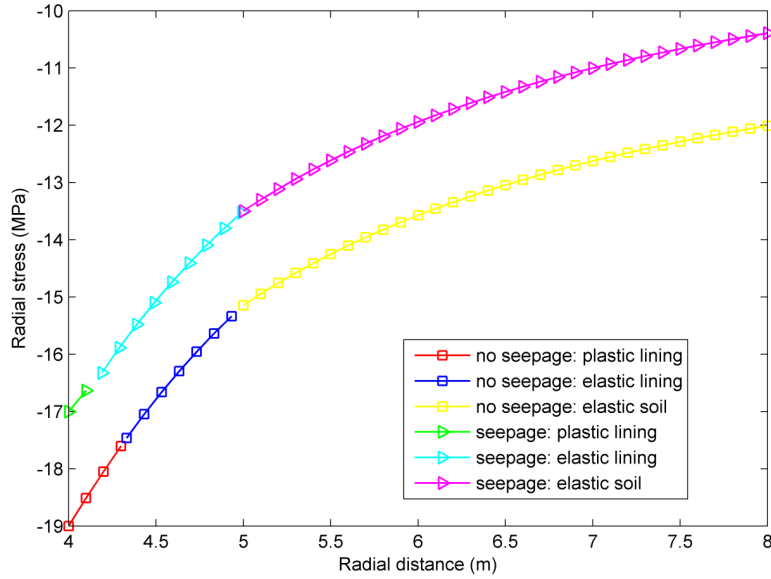
(a) Relationship between first critical pressure p_{cr1} and seepage water force p_{w0} (b) Relationship between second critical pressure p_{cr2} and seepage water force p_{w0}

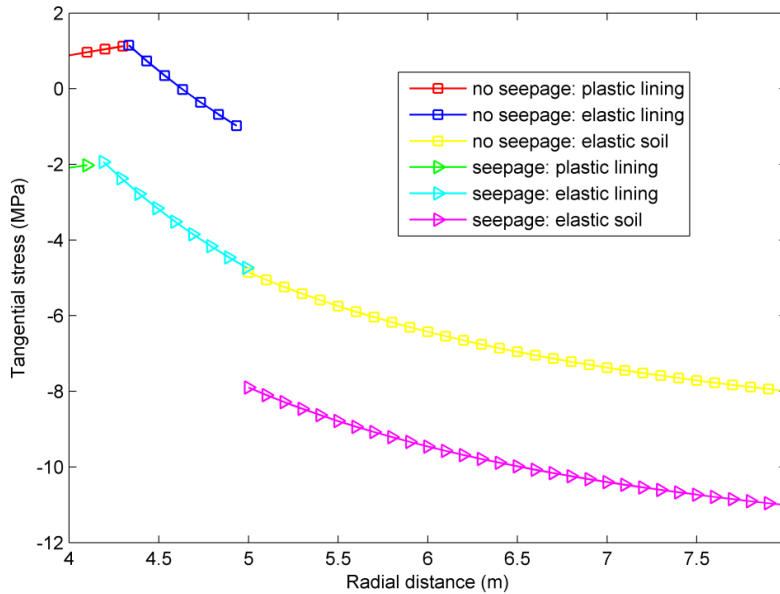
Figure 5: The influence of distant seepage water pressure on the first and second critical pressures

The laws of stress distribution of the lining and surrounding soil under given inner pressure are now analyzed, and the results obtained by considering seepage water pressure are compared with those when this pressure is ignored. Given inner pressure $p_a=19\text{MPa}$, the plastic radius is 4.19 m according to Eq. (21). According to the first and third formulae of Eq. (12) and Eq. (19), the curve of radial stress distribution can be given. Compared with the results when seepage water pressure is considered, the radial

stress has clearly decreased (see Fig. 6). Similarly, according to the second and fourth formulae of Eqs. (12) and (19), the curve of tangential stress distribution can be given, and is clearly larger than that when seepage water pressure is not considered (see Fig. 6).



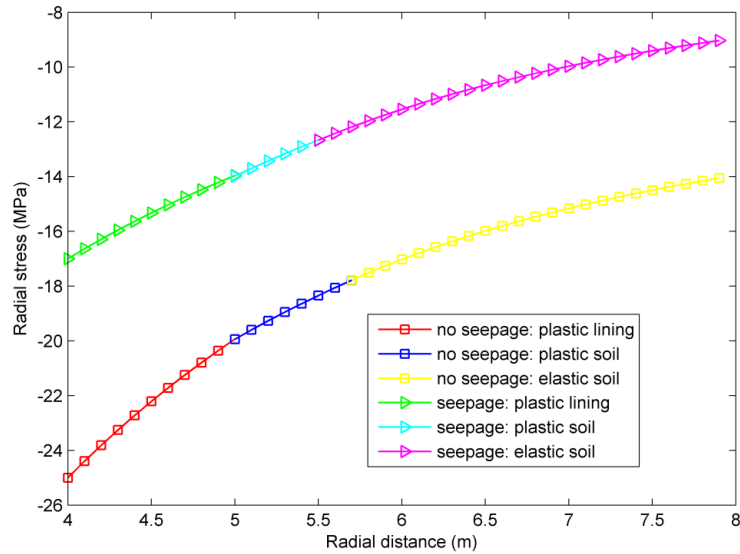
(a) Radial stress distribution contrast with and without seepage



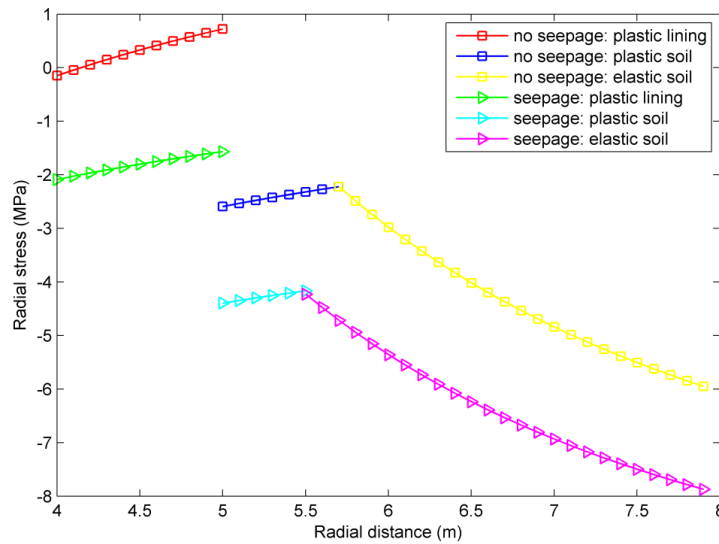
(b) Tangential stress distribution contrast with and without seepage

Figure 6: The influence of seepage force on stress distribution of lining and soil ($p_a = 19$ MPa)

Given inner pressure $p_a=19\text{MPa}$, the plastic radius is 5.50 m according to Eq. (24). Considering the seepage force, according to Eq. (22) and Lamé's solution, the curves of the radial and tangential stress distributions are given by Fig. 7. Compared with Fig. 6, the higher the inner pressure, the more prominent the influence of seepage water pressure on radial stress distribution, while the change in tangential stress is not prominent.



(a) Radial stress distribution contrast with and without seepage



(b) Tangential stress distribution contrast with and without seepage

Figure 7: The influence of seepage force on stress distribution of lining and soil ($p_a = 25 \text{ MPa}$)

The above calculation and analysis show that it is necessary to select the maximum principal stress reasonably according to different periods of tunnel construction and service, and the mechanism of the influence of seepage water pressure on stress on the tunnel changes.

6 Conclusions

Based on previous studies, this paper studied the effect of the seepage force on elastoplastic behavior of a tunnel with lining during construction and service. The maximum principle stress may change under different loads, and lead to differences in the elastoplastic behaviors of the surrounding soil and lining.

Owing to different distributions of internal pressure, the mechanisms of plastic failure of the tunnel's lining structure and surrounding soil change. The lining and surrounding soil entering the yield state generally encounter the following two situations: Support resistance during construction is insufficient to resist in-situ stress unloading caused by stratum disturbance, and the plastic failure of the lining structure (and part of the surrounding soil) occurs owing to excessive inner support resistance or pressure distribution in the tunnel. Methods to calculate the first, second, and third critical pressures were given. The stress field and plastic radius were determined by choosing appropriate calculation formulae according to the state of inner pressure distribution. Using an example the following was noted:

- (1) The mechanism of influence of seepage water pressure on plastic radius varied in the construction and service periods of the tunnel. During tunnel construction, the seepage water pressure promoted the plastic zone development of the lining and surrounding soil: That is, under the same inner pressure, the plastic radius was larger when the effect of seepage water pressure was considered. During the service period, however, with increasing inner pressure, the maximum principal stresses in the lining and surrounding soil changed into tangential stress while the seepage water pressure inhibited plasticity. The expansion of the plastic radius decreased when seepage water pressure was considered.
- (2) The first critical pressure increased with an increase in seepage water pressure. During construction, the inner support pressure of the tunnel needed to provide greater reaction force when the groundwater head was large. When the support force reached the first critical pressure, the development of plastic zone was theoretically restrained.
- (3) Considering the effect of seepage water pressure, the radial stress distribution was clearly different. Using inner pressure and comparing the results with those when the effect of seepage water pressure was ignored showed that the radial stress distribution when this pressure was considered was significantly reduced. The higher the inner pressure, the more obvious the influence of seepage water pressure on the radial stress distribution.
- (4) The influence mechanism of seepage water pressure on the stress distribution of the lining and surrounding soil also changed in different periods of tunnel construction and service, as did the mode of influence of seepage water pressure on the plastic radius and critical inner pressure of the tunnel.

Acknowledgments: This work was supported by the National Natural Science Foundation of China (Grant Nos. 51278467, 2015M582204 and 2016T90681).

References

- Atkinson, J. H.; Mair, R. J.** (1983): Loads on leaking and watertight tunnel lining, sewers and buried pipes due to groundwater. *Geotechnique*, vol. 33, no. 3, pp. 341-344.
- Bobet, A.** (2003): Effect of pore water pressure on tunnel support during static and seismic loading. *Tunnelling and Underground Space Technology*, vol. 18, no. 4, pp. 377-393.
- Brown, E. T.; Bray, J. W.; Ladanyi, B.; Hoek, E.** (1983): Ground response curve for rock tunnels. *Journal of Geotechnical Engineering*, vol. 109, no. 1, pp. 15-39.
- Carranza-Torres, C.** (2004): Elasto-plastic solution of tunnel problems using the generalized form of the Hoek-Brown failure criterion. *International Journal of Rock Mechanics and Mining Sciences*, vol. 41, no. 4, pp. 629-639.
- Carranza-Torres, C.; Fairhurst, C.** (1999): The elasto-plastic response of underground excavations in rock masses that satisfy the Hoek-Brown failure criterion. *International Journal of Rock Mechanics and Mining Sciences*, vol. 36, no. 6, pp. 777-809.
- Carranza-Torres, C.; Fairhurst, C.** (2000): Application of the convergence-confinement method of tunnel design to rock masses that satisfy the Hoek-Brown failure criterion. *Tunnelling and Underground Space Technology*, vol. 15, no. 2, pp. 187-213.
- Fernandez, G.; Alvarez, T. A.** (1994): Seepage-induced effective stresses and water pressures around pressure tunnels. *Journal of Geotechnical Engineering*, vol. 120, no. 1, pp. 108-128.
- Hamdia, K. M.; Ghasemi, H.; Zhuang, X. Y.; Alajlan, N.; Rabczuk, T.** (2018): Sensitivity and uncertainty analysis for flexoelectric nanostructures. *Computer Methods in Applied Mechanics and Engineering*, vol. 337, pp. 95-109.
- Hamdia, K. M.; Silani, M.; Zhuang, X. Y.; He, P. F.; Rabczuk, T.** (2017): Stochastic analysis of the fracture toughness of polymeric nanoparticle composites using polynomial chaos expansions. *International Journal of Fracture*, vol. 206, pp. 215-227.
- Jiang, Y.; Yaneda, H.; Tanabashi, Y.** (2001): Theoretical estimation of loosening pressure on tunnels in soft soils. *Tunnelling and Underground Space Technology*, vol. 16, no. 2, pp. 99-105.
- Lee, I. M.; Nam, S. W.** (2001): The study of seepage forces acting on the tunnel lining and tunnel face in shallow tunnels. *Tunnelling and Underground Space Technology incorporating Trenchless Technology Research*, vol. 16, no. 1, pp. 31-40.
- Li, X. X.; Cai, Y. C.; Zhuang, X. Y.; Zhu, H. H.** (2009): Design of permeable lining for high pressure hydraulic tunnel. *Rock and Soil Mechanics*, vol. 30, no. 5, pp. 1403-1408 (In Chinese).
- Lu, A. Z.; Xu, G. S.; Sun, F.; Sun, W. Q.** (2010): Elasto-plastic analysis of a circular tunnel including the effect of the axial in situ stress. *International Journal of Rock Mechanics and Mining Sciences*, vol.47, no. 1, pp. 50-59.
- Wood, A. M. M.** (1975): The circular tunnel in elastic ground. *Geotechnique*, vol. 25, no. 1, pp. 115-127.
- Oreste, P. P.** (2003): Analysis of structural interaction in tunnels using the convergence-confinement approach. *Tunnelling and Underground Space Technology*, vol. 18, no. 4,

pp. 347-363.

Rabczuk, T.; Belytschko, T. (2004): Cracking particles: a simplified mesh-free method for arbitrary evolving cracks. *International Journal for Numerical Methods in Engineering*, vol. 61, pp. 2316-2343.

Rabczuk, T.; Zi, G.; Bordas, S.; Nguyen-Xuan, H. (2010): A simple and robust three-dimensional cracking-particle method without enrichment. *Computer Methods in Applied Mechanics and Engineering*, vol. 199, pp. 2437-2455.

Ren, H. L.; Zhuang, X. Y.; Cai, Y. C.; Rabczuk, T. (2016): Dual-horizon peridynamics. *International Journal for Numerical Methods in Engineering*, vol. 108, pp. 1451-1476.

Ren, H. L.; Zhuang, X. Y.; Rabczuk, T. (2017): Dual-horizon peridynamics: a stable solution to varying horizons. *Computer Methods in Applied Mechanics and Engineering*, vol. 318, pp. 762-782.

Ren, Q. W.; Zhang, H. C. (2001): A modification of Fanner formula. *Journal of Hohai University*, vol. 29, no. 6, pp. 109-111 (In Chinese).

Sharan, S. K. (2003): Elastic–brittle–plastic analysis of circular openings in Hoek-Brown media. *International Journal of Rock Mechanics and Mining Sciences*, vol. 40, no. 6, pp. 817-824.

Shin, Y. J.; Kim, B. M.; Shin, J. H.; Lee, I. M. (2010): The ground reaction curve of underwater tunnels considering seepage forces. *Tunnelling and Underground Space Technology*, vol. 25, no. 4, pp. 315-324.

Stille, H.; Holmberg, M.; Nord, G. (1989): Support of weak rock with grouted bolts and shotcrete. *International Journal of Rock Mechanics and Mining Sciences & Geomechanics Abstracts*, vol. 26, no. 1, pp. 99-113.

Timoshenko, S. P.; Goodier, J. N. (1969): *Theory of Elasticity*. McGraw-Hill, New York.

Xie, H. Q. (1994): *Study on Multi-Field Coupled Effects of Heat, Liquid and Solid in Tunnel Works (Ph.D. thesis)*. Southwest Jiaotong University, Chengdu (In Chinese).

Zhou, S. W.; Rabczuk, T.; Zhuang, X. Y. (2018): Phase field modeling of quasi-static and dynamic crack propagation: COMSOL implementation and case studies. *Advances in Engineering Software*, vol. 122, pp. 31-49.

Zhou, S. W.; Xia, C. C. (2018): Propagation and coalescence of quasi-static cracks in Brazilian disks: an insight from a phase field model. *Acta Geotechnica*.

Zhou, S. W.; Zhuang, X. Y.; Rabczuk, T. (2018): A phase-field modeling approach of fracture propagation in poroelastic media. *Engineering Geology*, vol. 240, pp. 189-203.

Zhou, S. W.; Zhuang, X. Y.; Rabczuk, T. (2019): Phase-field modeling of fluid-driven dynamic cracking in porous media, *Computer Methods in Applied Mechanics and Engineering*.

Zhou, S. W.; Zhuang, X. Y.; Zhu, H. H.; Rabczuk, T. (2018): Phase field modelling of crack propagation, branching and coalescence in rocks. *Theoretical and Applied Fracture Mechanics*, vol. 96, pp. 174-192.